Superconductivity in Li-doped α-rhombohedral boron

T. Nagatochi,[1] H. Hyodo,[2] A. Sumiyoshi,[1] K. Soga,[2] Y. Sato,[3] M. Terauchi,[3] F. Esaka,[4] and K. Kimura[1]

[1]*Department of Advanced Materials Science, The University of Tokyo, Japan*

[2]*Department of Materials Science and Technology, Tokyo University of Science, Japan*

[3]*Institute for Multidisciplinary Research for Advanced Materials, Tohoku University, Japan*

[4]*Japan Atomic Energy Agency, Japan*

(Received 8 December 2010; published 16 May 2011)

Metal transition and superconductivity were observed in Li-doped α-rhombohedral boron (α-B_{12}). The authors have established a purification method and obtained a large amount of high-purity α-B_{12} powder. Li doping into purified α-B_{12} was attempted by vapor diffusion processing (VDP) in a Mo or Ta tube. Li-doped α-B_{12} contained metallic glittering particles. Meissner effects were observed in such a compound with the nominal composition Li_xB_{12} ($x = 1.0$, 1.4, 1.5, 1.7, or 2.5) ($T_c = 3.2$–7 K). As for $Li_{2.5}B_{12}$, the temperature dependence of its electrical conductivity indicates a metallic character and its electrical resistivity drop is detected near the Meissner temperature. The existence of Li and Fermi edges in Li-doped α-B_{12} crystals was verified by transmission electron microscopy-electron energy loss spectroscopy (TEM-EELS). Lattice expansion, which is a well-known indicator of metal doping into a crystal, was also observed. Thus, Li doping into α-B_{12} was successfully achieved. Our work also suggests that it is possible to dope a larger amount of Li into α-B_{12} and to increase its T_c.

DOI: 10.1103/PhysRevB.83.184507 PACS number(s): 74.70.Ad, 61.72.U−, 81.05.Je, 81.20.Ym

I. INTRODUCTION

B-rich solids including elemental boron (B), such as α- and β-rhombohedral (α-B_{12} and β-B_{105}, respectively), α-tetragonal (α-B_{50}), and γ-orthorhombic (γ-B_{28}) B's, have a framework crystalline structure built up from B_{12} icosahedra.[1–4] They are called boron-icosahedral cluster solids (B-ICSs). One of the remarkable characteristics of B-ICSs is the high degeneracy of their electronic states due to the high symmetry of icosahedra. Such degeneracy brings a relatively high density of states (DOS) and if one can adjust the Fermi energy (E_F) to this high-DOS position, B-ICSs could be a high-T_c superconductor.[5–8] Another remarkable character of B-ICSs is their comparatively large interstitial cites, therefore, there are some attempts to dope other elements into B-ICSs, aiming at the adjustment of E_F.[9–12]

In spite of many experimental efforts,[9–12] there is still no reliable report on superconductivity or metal transition in metal-doped B-ICSs. We reported the possibility of superconductivity in Li-doped α-B_{12} in our previous paper.[10] However, because its volume fraction was only 0.02% and x-ray analysis could not reveal evidence of Li doping, it is doubtful whether superconductivity originated from Li-doped α-B_{12}. There are two problems in the previous experiments. The first problem is that the crystallized α-B_{12} powder included impurity phases, that is, B_6O, β-B_{105}, and amorphous boron (am-B), and these impurity phases covered the surface of α-B_{12} particles and obstructed effective Li doping [Fig. 1(a)]. The second problem is that Li reacted not only with α-B_{12} but also with the quartz tube used for the sealing.

In this study we solved these problems by removing impurity phases by chemical treatment and by improving doping processes using a Ta or Mo tube, and report on the discovery of a superconductor in the Li-doped α-B_{12} system.

II. EXPERIMENTAL

Raw α-B_{12} powder for refining was prepared by annealing 4N purity am-B at 1200 °C for 50 h.[10,13] X-ray diffraction analysis with Cu$K\alpha$ radiation showed that α-B_{12} is the main phase of the annealed am-B powder but that some impurity phases (i.e., β-B_{105}, B_6O, and am-B phases) are contained [as shown in Fig. 2(a)]. B_6O was generated from oxides (mainly B_2O_3) originally included in the 4N purity am-B. β-B_{105} and am-B were generated and remained, respectively, because of the narrow crystallization temperature range of α-B_{12}.[10,13] Figure 1(a) shows a SEM image of the annealed am-B powder. Crystallized α-B_{12} particles are covered with impurity phases, which should interrupt effective Li doping. To dope Li effectively, we dissolved the impurity phases β-B and am-B on these crystallized α-B_{12} particles by ultrasonic vibration in nitric acid for 100 min. After neutralization and centrifugation, β-B and am-B were completely removed, but B_6O remained. A liquid mixture was prepared by adding 5 ml of pure water, 20 ml of ethanol and 20 ml of glycerol to 0.1 g of nitric acid-processed α-B_{12} powder. The liquid mixture was then ultrasonically vibrated and centrifuged for 5 min at 3700 G. As a result, the liquid phase was separated into three layers and B_6O was easily removed. Figure 1(b) shows a FE-SEM image of the purified α-B_{12} powder. No impurity is observed on the surface of α-B_{12}. This means that effective Li doping is attainable. Figure 2(b) shows the XRD patterns of the purified α-B_{12} powder. No impurity phase was observed. Therefore we successfully obtained high-purity α-B_{12} powder. The productivity of this refining process is approximately 20%. Some of the purified α-B_{12} powder was used to form cylindrical pellets by spark plasma sintering (SPS) for the evaluation of electrical conductivity.

The Li doping of the purified powder and pellets was attempted by a vapor diffusion process (VDP), which is a

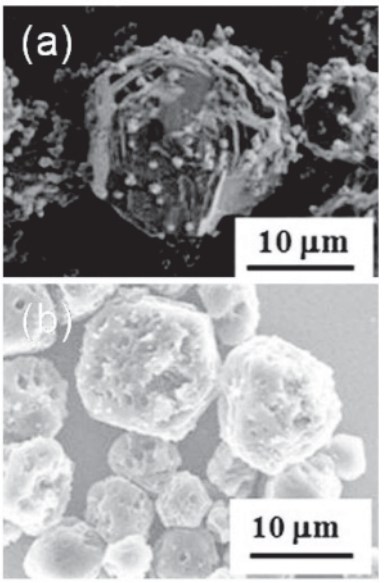

FIG. 1. SEM images of (a) annealed am-B powder. The surface of α-B_{12} crystals is covered with impurity phases. The small particles are B_6O polycrystals. (b) Purified α-B_{12} powder. Clean and bare surfaces of α-B_{12} crystals are shown.

similar method used in the previous studies.[9–12] Li doping was improved using a Mo or Ta tube, which hardly reacts with Li, instead of a quartz tube. Purified α-B_{12} powder and pellets were placed in a hexagonal boron nitride crucible and sealed in a Mo or Ta tube with Li by arc welding then annealed at several temperatures between 1173 and 1673 K for 0.2–100 h.

III. RESULTS AND DISCUSSION

Some of the Li-doped samples contained metallic glittering particles. Meissner effects were observed in the samples with nominal composition Li_xB_{12} (x = 1.0, 1.4, 1.5, 1.7, or 2.5) (T_c = 3.2∼7 K), as shown in Fig. 3 for a typical example and as summarized in Table I. The volume fractions estimated from ZFC curves were scattered from 0.63% to 13.82%. The

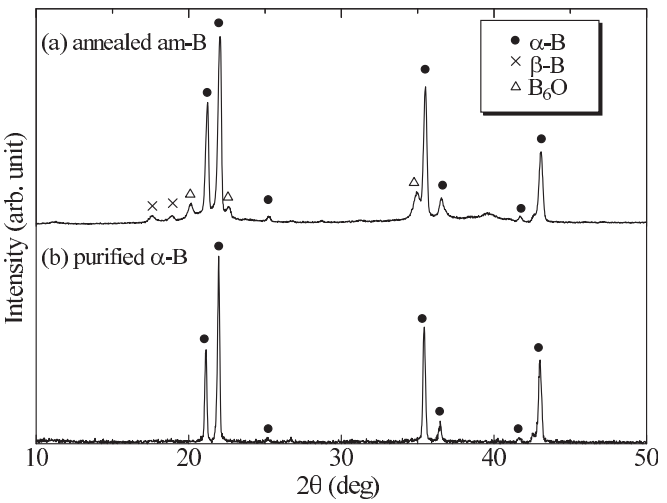

FIG. 2. XRD patterns of (a) annealed am-B powder and (b) purified α-B_{12} powder.

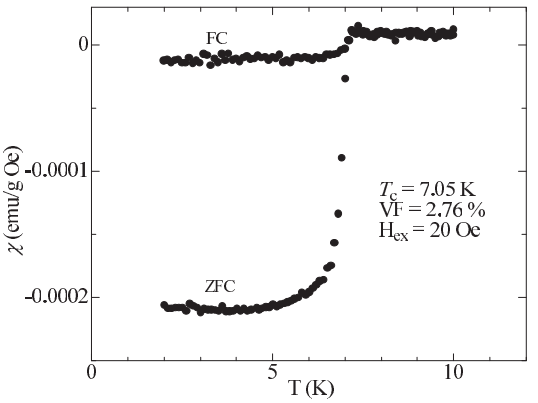

FIG. 3. Temperature dependence of magnetic susceptibility χ of $Li_{1.7}B_{12}$.

differences in T_c may be accounted for by the different site occupancies of the dopant Li. Theoretical studies have revealed that the effect of Li doping is nearly rigid-band-model-like.[5,7,8] Therefore one of the parameter of T_c, the DOS at the Fermi energy [$N(E_F)$], varies in proportional to the amount of doped Li and T_c may change. The site occupancies of the Li will be discussed later. Figure 4 shows the temperature dependence of the electrical conductivity (σ) of Li-doped α-B_{12}. σ increases with increasing nominal composition of Li. $Li_{2.5}B_{12}$ shows metallic electrical conductivity and an electrical resistivity drop near the Meissner temperature (T_c = 6.62 K), as shown in Figs. 4 and 5, respectively. The reason for imperfect resistivity drop is possibly the nonuniformity of the doping into the interstitial sites of α-B_{12}.

The secondary ion mass spectroscopy (SIMS) of Li-doped α-B_{12} pellets revealed that there are only small differences between their nominal and analyzed compositions. Therefore it is guaranteed that stocked Li was completely diffused on average in each pellet by VDP. Transmission electron microscopy-electron energy loss spectroscopy (TEM-EELS) detected Li and the Fermi edges in some Li-doped α-B_{12} fine particles ($Li_{2.5}B_{12}$-2 in Fig. 6). Although, in most of the other particles, a chemical shift of the 1s electron-excitation

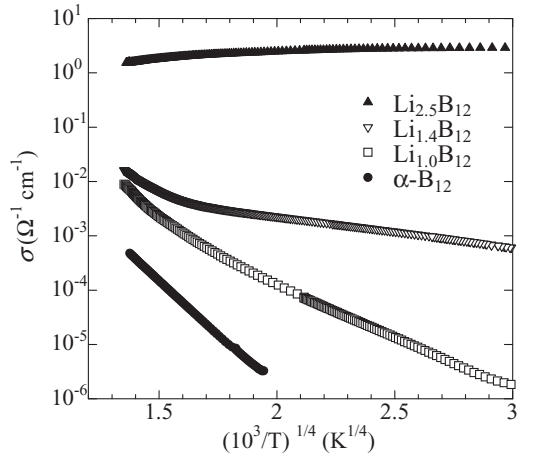

FIG. 4. Temperature dependences of electrical conductivities σ of α-B_{12}, $Li_{1.0}B_{12}$, $Li_{1.4}B_{12}$, and $Li_{2.5}B_{12}$. σ is plotted according to the formula of variable-range hopping conduction.

TABLE I. Nominal compositions, superconducting transition temperatures (T_c's), volume fraction (VFs), and results of performed analysis of Li-doped α-B_{12} samples. χ, σ, SOR XRD, SIMS, and TEM-EELS means magnetic susceptibility, electrical conductivity, synchrotron orbital radiation x-ray diffraction, secondary ion microscope spectroscopy, and transmission electron microscopy-electron energy loss spectroscopy measurements, respectively. T_c and VF are estimated by χ measurement. The inclusion of two T_c's for one sample means that two superconductivity transfer steps were observed in one spectrum. Powder and bulk samples with equal nominal compositions were annealed at the same time.

Nominal composition	Sample type	Container material	TA (K)	VF (%)	Analysis
$Li_{1.0}B_{12}$	Powder	Ta	3.24	0.19	χ
$Li_{1.0}B_{12}$	Bulk	Ta	–	–	σ
$Li_{1.4}B_{12}$	Powder	Ta	3.20 and 3.8 1	1.54	χ, SOR XRD
$Li_{1.4}B_{12}$	Bulk	Ta	–	–	σ , SIMS
$Li_{1.5}B_{12}$	Powder	Mo	4.00 and 5.60	13.82	χ
$Li_{1.7}B_{12}$	Powder	Mo	7.05	2.76	χ
$Li_{2.5}B_{12}$	Powder	Mo	3.19 and 5.21	0.63	χ, TEM-EELS
$Li_{2.5}B_{12}$	Powder	Mo	7.02	0.38	χ
$Li_{2.5}B_{12}$	Bulk	Mo	6.62	–	σ, SIMS

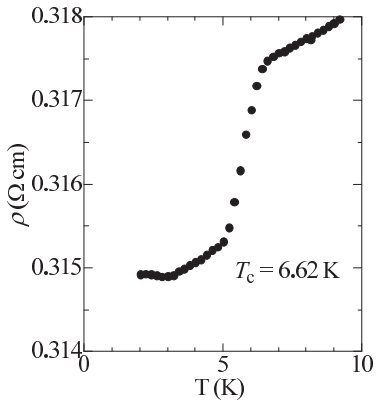

FIG. 5. Temperature dependence of electrical resistivity ρ of bulk $Li_{2.5}B_{12}$.

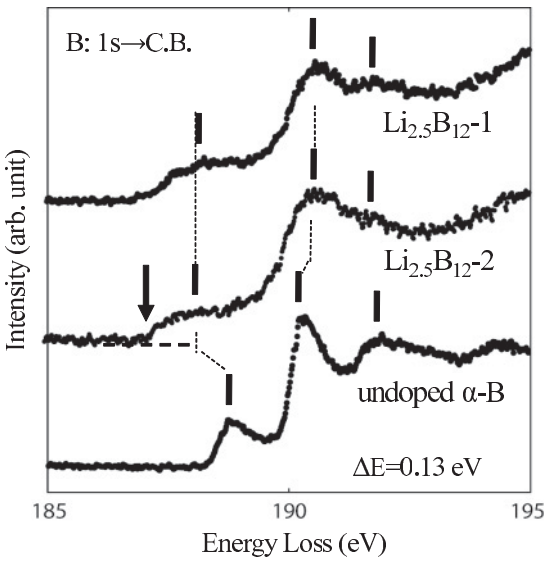

FIG. 6. EELS profiles of undoped and Li-doped α-B_{12}s.The arrow indicates the Fermi edge and the bars correspond to the peaks of each spectrum.

spectra, which corresponds to the DOS of the conduction bands, was observed, no Fermi edge was observed ($Li_{2.5}B_{12}$-1 in Fig. 6). This means that most of the minute Li-doped α-B_{12} crystals were electron doped; however, the number of the doped carriers was not sufficient for the metal transition. Therefore, a well-Li-doped superconducting (SC) phase and some Li-doped semiconducting phases were formed, resulting in small volume fractions of the SC phase.

The site occupancies and lattice constants were calculated using the powder XRD patterns obtained at the SPring-8 synchrotron radiation facility. Program RIETAN2000 was used for the Rietveld refinement.[14] Figure 7 shows the results of the Rietveld analysis of the XRD data for $Li_{1.40}B_{12}$ (T_c = 3.2 and 3.8 K) doped with Li in a Ta tube. No possible compound (Ta, TaB, or TaB_2) with a similar T_c was observed in the XRD patterns. Table II shows the result of the Rietveld refinement and Table III shows a comparison of the site occupancies and lattice constants obtained with previous experimental values of pristine α-B_{12} and theoretical values. The experimental composition of the $Li_{1.40}B_{12}$ calculated by Rietveld refinement is $Li_{0.30}B_{12}$, which is found different

TABLE II. Crystal data and refined structural parameters for the $Li_{1.4}B_{12}$ sample. R_{wp} and R_I are reliability factors. a and c are the lattice constants of the hexagonal unit cell. g is the occupancy at each atomic site. x, y, and z are fractional coordinates. The isotropic atomic displacement parameter was fixed at 0.5 upon the fitting.

$Li_{1.4}B_{12}$				
R_{wp} = 2.86%			R_I = 4.82%	
Lattice constant	a = 4.9457(1)		c = 12.6420(1)	
Site	g	x	y	z
Bl (p)	1	0.7848(2)	l-x	0.2242(1)
B2 (e)	1	0.8623(2)	l-x	0.3570(1)
Li1	0.212(1)	0	0	0.5
Li2	0.022(1)	0	0	0.25

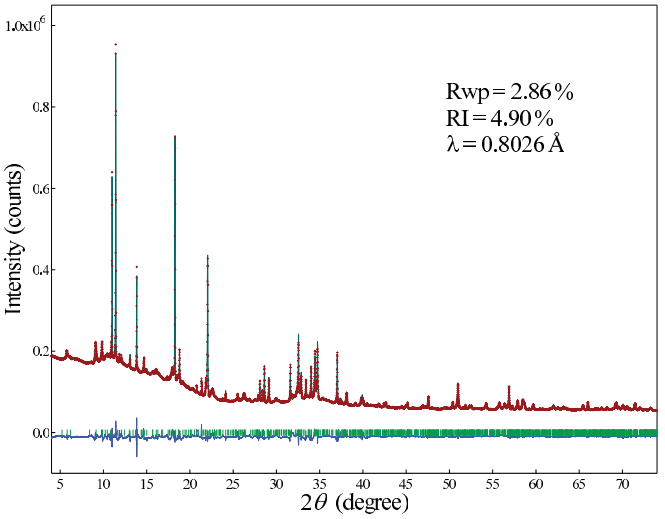

FIG. 7. (Color online) XRD patterns of $Li_{1.40}B_{12}$ acquired at SPring-8 and residuals of Rietveld refinement.

from the composition of $Li_{1.26}B_{12}$ determined by SIMS. This disagreement in composition means that diffused Li was not completely doped into and ionized in the α-B_{12} crystals. The bulk density of the α-B_{12} pellets sintered by SPS is nearly 70%; therefore, most of the diffused Li would localize in pores and would not contribute to carrier doping. In other words, Rietveld analysis detected only doped Li in the doping sites but SIMS measurement detected all Li including oxides in the pore of pellets. Some Li exists on the surface of pores in the sample. Li doping is not uniform, and highly electron-doped regions (SC) and not sufficiently doped regions (semiconductor) are mixed. Hence, the path of the superconducting current was not completely connected and residual resistance remained (as shown in Fig. 5).

Small residuals in Fig. 7, which indicated a highly Li-doped α-B_{12} phase (SC), were observed on the smaller-θ side of the $Li_{1.4}B_{12}$ ($Li_{0.30}B_{12}$) XRD peaks. This doping inequality is consistent with the TEM-EELS analysis. A clear lattice expansion was observed in $Li_{1.4}B_{12}$ ($Li_{0.30}B_{12}$), but the expansion ratios were smaller than the theoretical values [a = 0.75% (theory: 0.47%), c = 0.56% (theory: 2.76%)] as shown in TABLE II. This was caused by the low O-site occupancy for $Li_{1.4}B_{12}$ ($Li_{0.3}B_{12}$). This low occupancy means that more space for Li is remaining. The effect of Li doping is considered to be nearly the same as that in the rigid-band model. Therefore, there is a possibility of obtaining higher T_c by doping a larger amount of Li into α-B_{12} using a catalyst or a high-pressure technique.[15]

TABLE III. Experimental and theoretical lattice constants of the hexagonal unit cell and occupancies of Li doping sites. Expansion ratios are calculated from the lattice constants before and after Li doping.

Composition		Lattice constant (Å)		Occupancy (%)	
Nominal	Analytical	a (Å)	c (Å)	Li (O)	Li (T_d)
-	B_{12}[16]	4.9089(1)	12.5716(1)	0	0
$Li_{1.4}B_{12}$	$Li_{0.3}iB_{12}$	4.9457(1)	12.6420(1)	0.212	0.044
Expansion ratio (%)		0.7497	0.5600	-	-
-	B_{12}[8]	4.857	12.270	0	0
-	$Li_{1.0}B_{12}$[8]	4.880	12.609	1	0
Expansion ratio (%)		0.4735	2.7628	-	-

TABLE IV. Comparisons of B_{12} icosahedra distortion between previous experimental study of pure α-B_{12}[16] and this study. Lattice parameters are represented by the rhombohedral unit cell. The distortion ratios before and after Li doping are shown in parentheses.

	B_{12}[16]	$Li_{1.4}B_{12}$ ($Li_{0.3}B_{12}$)
Angle (deg)		
α_{Rhomb}	58.05	58.13(0.14%)
p-C-p	61.59	61.67(0.13%)
p-C-e	64.04	63.90(−0.22%)
e-C-e	63.25	63.06(−0.30%)
Distance (Å)		
α_{Rhomb}	5.059	5.090(0.62%)
C-p	1.713	1.713(0.01%)
C-e	1.702	1.700(−0.10%)
p-p	1.754	1.756(0.13%)
p-e	1.817	1.816(−0.03%)
p-e	1.811	1.806(−0.24%)
e-e	1.785	1.778(−0.38%)
Intercluster p-p	1.641	1.672(1.89%)

Table IV shows comparisons of rhombohedral lattice angle, lattice constants, intracluster B-B bonding, and intercluster B-B bonding between pristine α-B_{12}[16] and $Li_{1.4}B_{12}$ ($Li_{0.3}B_{12}$) in this work. C sites are the center of B_{12} icosahedra (0, 0, 0). The B atoms that have an intercluster two-center bond are called "p" which means polar. In contrast, the B atoms that have intercluster three-center bond are called "e", which means equatorial. These p and e sites are equal to B1 (p) and B2 (e) in Table II, respectively. In Table IV the comparisons between pristine α-B_{12} in the previous work and $Li_{1.4}B_{12}$ ($Li_{0.3}B_{12}$) in this work confirmed that the rhombohedral lattice angle α and intracluster bonding distance and angle hardly changed even after Li doping (insertion). In contrast to intracluster bonding distances, the intercluster p-p bonding distance was increased by Li insertion.

IV. CONCLUSIONS

In this study we report the superconducting transition of Li-doped α-B_{12} crystals for the first time, which was realized by the purification method that removes impurity phases in the α-B_{12} crystallized from amorphous boron. Meissner effects were observed with nominal compositions of Li_xB_{12} (x = 1.0, 1.4, 1.5, 1.7, 2.5) (T_c = 3.2∼7 K). The temperature dependence of the electrical conductivity of α-B_{12} is improved in proportion to the amount of doped Li. TEM-EELS measurement detected Li and Fermi edges in Li-doped α-B_{12} fine particles, but doping inequality was also observed. Lattice expansion and Li were observed by the Rietveld analysis of the XRD patterns of Li-doped α-B_{12} at SPring-8. Therefore, Li doping into α-B_{12} was successfully achieved for the first time. The depth profiles of Li by SIMS revealed that almost all the stacked Li diffused into the pellets, but a large amount of Li must have localized in pores and does not contribute to the carrier doping. Our work

also demonstrates that it is possible to dope a larger amount of Li into α-B_{12} and increase its T_c.

ACKNOWLEDGMENTS

The authors would like to thank Mr. Yamauchi in the Electromagnetic Measurements Laboratory, Institute for Solid State Physics, The University of Tokyo for valuable technical support. This work is partly supported by Scientific Research on Priority Areas of New Materials Science Using Regulated Nano Spaces, KAKENHI No. 19051005 from MEXT. The synchrotron radiation experiments were performed at the BL02B2 station of SPring-8 with the approval of the Japan Synchrotron Radiation Research Institute (Proposal No. 2007B1659 and No. 2009A1325).

[1] I. Higashi, AIP Conf. Proc. **140**, 1 (1985).
[2] Z. Wang, Y. Shimizu, T. Sasaki, K. Kawaguchi, K. Kimura and N. Koshizaki, Chem. Phys. Lett. **368**, 663 (2003).
[3] A. R. Oganov, J. Chen, C. Gatti, Y. Ma, Y. Ma, C. W. Glass, Z. Liu, T. Yu, O. O. Kurakevych, and V. L. Solozhenko, Nature (London) **457**, 07736 (2009).
[4] E. Zarechnaya, L. Dubrovinsky, N. Dubrovinskaia, N. Miyajima, Y. Filinckuk, D. Chernyshov, and V. Dmitriev, Sci. Technol. Adv. Mater. **9**, 044209 (2008).
[5] S. Gunji, and H. Kamimura, Phys. Rev. B **54**, 13665 (1996).
[6] M. Calandra, N. Vast, and F. Mauri, Phys. Rev. B **69**, 224505 (2004).
[7] W. Hayami, T. Tanaka, and S. Otani, J. Phys. Chem. A **109**, 11975 (2005).
[8] H. Dekura, K. Shirai, and H. Katayama-Yoshida, J. Phys. Condens. Matter **19**, 365241 (2007).
[9] H. Matsuda, T. Nakayama, K. Kimura, Y. Murakami, H. Suematsu, M. Kobayashi, and I. Higashi, Phys. Rev. B **52**, 6102 (1995).
[10] K. Soga, A. Oguri, S. Araake, M. Terauchi, A. Fujiwara, and K. Kimura, J. Solid State Chem. **177**, 498 (2004).
[11] K. Kirihara, H. Hyodo, H. Fujihisa, Z. Wang, K. Kawaguchi, Y. Shimizu, T. Sasaki, N. Koshizaki, K. Soga, and K. Kimura, J. Solid State Chem. **179**, 2799 (2006).
[12] H. Hyodo, S. Araake, S. Hosoi, K. Soga, Y. Sato, M. Terauchi, and K. Kimura, Phys. Rev. B **77**, 024515 (2008).
[13] S. O. Shalamberidze, G. I. Kalandadze, D. E. Khulelidze, and B. D. Tsurtsumia, J. Solid State Chem. **154**, 199 (2000).
[14] F. Izumi, and T. Ikeda, Mater. Sci. Forum **321**, 198 (2000).
[15] K. Shirai, H. Dekura, and A. Masago, J. Phys. Conf. Ser. **176**, 012001 (2009).
[16] S. Hosoi, H. Kim, T. Nagata, K. Kirihara, K. Soga, K. Kimura, K. Kato, and M. Takata, J. Phys. Soc. Jpn. **76**, 044602 (2006).